Bioorganic & Medicinal Chemistry 28 (2020) 115737

Contents lists available at ScienceDirect

Bioorganic & Medicinal Chemistry

journal homepage: www.elsevier.com/locate/bmc

New BODIPYs for photodynamic therapy (PDT): Synthesis and activity on human cancer cell lines

Enrico Caruso[a,1], Miryam C. Malacarne[a,1,2], Emanuela Marras[a], Ester Papa[b], Linda Bertato[b], Stefano Banfi[a], Marzia B. Gariboldi[a,*]

[a] Department of Biotechnology and Life Sciences (DBSV). University of Insubria, Via J.H. Dunant 3, 21100 Varese (VA), Italy
[b] Department of Theoretical and Applied Sciences (DiSTA). University of Insubria, Via J.H. Dunant 3, 21100 Varese (VA), Italy

ARTICLE INFO

Keywords:
Photodynamic therapy
BODIPY
Cell death
ROS
Cellular migration

ABSTRACT

A new class of compounds based on the 4,4-difluoro-4-bora-3a,4a-diaza-s-indacene core, known as BODIPYs, has attracted significant attention as photosensitizers suitable for application in photodynamic therapy (PDT), which is a minimally invasive procedure to treat cancer. In PDT the combination of a photosensitizer (PS), light, and oxygen leads to a series of photochemical reactions generating reactive oxygen species (ROS) exerting cytotoxic action on tumor cells.

Here we present the synthesis and the study of the *in vitro* photodynamic effects of two BODIPYs which differ in the structure of the substituent placed on the *meso* (or 8) position of the dipyrrolylmethenic nucleus. The two compounds were tested on three human cancer cell lines of different origin and degree of malignancy.

Our results indicate that the BODIPYs are very effective in reducing the growth/viability of HCT116, SKOV3 and MCF7 cells when irradiated with a green LED source, whereas they are practically devoid of activity in the dark. Phototoxicity occurs mainly through apoptotic cell death, however necrotic cell death also seems to play a role. Furthermore, singlet oxygen generation and induction of the increase of reactive oxygen species also appear to be involved in the photodynamic effect of the BODIPYs. Finally, it is worth noting that the two BODIPYs are also able to exert anti-migratory activity.

1. Introduction

Photodynamic therapy (PDT) is an alternative modality for the treatment of neoplastic and non-malignant lesions in which the combination of a photosensitizing drug (PS), light and oxygen leads to a series of photochemical reactions generating reactive oxygen species (ROS), which are able to cause localized tissue damages.[1,2] Despite applications are growing, the use of PDT in clinical oncology is still limited, mainly due to a number of limitations, such as phototoxic and photoallergic adverse effects, PSs suboptimal tissue penetration, along with problems in obtaining appropriate PSs formulations and dosages.[3] Furthermore, the most clinically relevant PDT agents are cyclic tetrapyrroles (porphyrins, chlorins, and bacteriochlorins) which can require complex synthetic pathways or difficult chemical modifications to modulate their photophysical and biological properties.[4] Hence, the synthesis and characterization of new PSs are actively pursued by many laboratories.[3,5] These new PSs should possess improved properties to overcome the limitations described above and belong to non-porphyrin photosensitizers, that might be synthetized more easily.

In this respect, over the last decade, a new class of photosensitizers based on the 4,4-difluoro-4-bora-3a,4a-diaza-s-indacene core, commonly known as BODIPYs, has attracted considerable attention.[6–9] BODIPYs have been mainly used as fluorescent dyes and for various other applications.[8,10–12]. The potential use of BODIPYs in PDT has been supported by a number of favourable chemico-physical features that make these molecules ideal photosensitizers, such as tuneable hydrophilic/hydrophobic character, high molar extinction coefficients (generally associate to strong fluorescence), stability under different environmental conditions, resistance to photobleaching and high light-dark toxicity ratio.[7,13–15] However, some of these features could also exert detrimental effects; indeed, if on the one hand photodynamic activity may benefit from the high chemical stability of the BODIPYs, on the other hand low biodegradation processes might be associated with persistent skin photosensitization, by far longer the therapeutic

* Corresponding author at: Department of Biotechnology and Life Sciences (DBSV), University of Insubria, Via JH Dunant 3, Varese, Italy.
E-mail address: marzia.gariboldi@uninsubria.it (M.B. Gariboldi).
[1] The two authors contributed equally to this work.
[2] PhD student of the "Life Science and Biotechnology" course at University of Insubria.

https://doi.org/10.1016/j.bmc.2020.115737
Received 11 June 2020; Received in revised form 6 August 2020; Accepted 22 August 2020
Available online 29 August 2020
0968-0896/

necessity. As far as fluorescence is concerned, this property plays a fundamental role when BODIPYs are exploited as biological probes while it severely limits their use as photosensitizers, since it indicates that a large part of the energy absorbed upon excitation is lost through a process that does not favor the production of cell toxic reactive oxygen species. Therefore, when a photosensitizing action is required, high quantum efficiency of fluorescence should be inhibited. To this purpose, BODIPY structure needs to be modified using substituents with an appropriate oxidation potential.[8,16,17] Several studies focused on BODIPY core modifications to increase singlet oxygen generation showed that such substituents should possess unshared valence electron pairs to quench the fluorescence of photoexcited BODIPYs, thereby generating relatively long-lived triplet states. Following the interaction of these last species with $^3O_2$, high production of singlet oxygen is guaranteed.[7,18,19]

Another important practical aspect favoring the development of BODIPYs for PDT comes from their "one-pot" synthetic pathway. As a matter of fact, the general scheme of BODIPY synthesis involves the acid-catalyzed reaction, between pyrroles and aldehydes (or acyl chlorides), yielding dipyrrolylmethane which is first easily oxidized to dipyrrolylmethene with 2,3-dichloro-5,6-dicyano-1,4-benzoquinone (DDQ) and finally borinated with boron trifluoride ($BF_3 \cdot Et_2O$) in the presence of a tertiary amine.[20]

In this manuscript we report the synthesis of two BODIPY derivatives (compounds **3** and **4**) which differ in the length of the hydrocarbon chain located in position 4 (*para*) of the phenyl ring in position 8 (*meso*) of the dipyrromethenic core; in particular, compounds **3** and **4** bear a carbon chain of four or eight units respectively, which should confer different degrees of lipophilicity. This difference should allow to establish the existence of a correlation between the length of the alkyl chain and the photodynamic activity of the two BODIPYs. Furthermore, to make these BODIPY more versatile, allowing for example their attachment by covalent bonds to nanoparticles, each chain features a bromine atom in the terminal CH_2 group. This molecule functionalization has been previously utilized by our group to improve the *in vivo* bioavailability of porphyrinic derivatives.[21]

The *in vitro* photodynamic activity of these compounds was assessed on human cancer cell lines of different origin and degree of malignancy, namely the colon adenocarcinoma HCT116 cells, the ovarian cancer SKOV3 cells and the breast adenocarcinoma MCF7 cells, following irradiation with a low energy green LED light, as these molecules are characterized by intense absorbance in the 495–535 nm range. The ability of the BODIPYs to induce apoptotic and necrotic response, along with singlet oxygen and reactive oxygen species production, cellular uptake, and spontaneous cell migration inhibition, was also evaluated.

2. Results and discussion

2.1. Synthesis

The aromatic aldehydes, 4-[(4-bromobutyl)oxy]benzaldehyde (**1**) and 4-[(8-bromooctyl)oxy]benzaldehyde (**2**), used for the synthesis of the two BODIPYs were obtained by reacting the 4-hydroxybenzaldehyde and the appropriate alkyldibromide (1,4-dibromobutane or 1,8-dibromooctane), following the procedure reported in the literature[21] (Scheme 1).

The BODIPY derivatives were synthesized by condensation of aromatic aldehydes **1** or **2** with 2,4-dimethylpyrrole in the presence of catalytic amount of trifluoroacetic acid (TFA), following the general procedure described by Dost and Liu.[15,16] The subsequent addition of 2,3-dichloro-5,6-dicyano-1,4-benzoquinone (DDQ) oxidizes the dipyrrolylmethanes to the corresponding dipyrrolylmethenes, which are then treated with $BF_3{\cdot}Et_2O$ in the presence of Et_3N to obtain the desired BODIPYs. Compounds **3a** and **4a** were isolated as pure solid after a single chromatographic step of purification (SiO_2, CH_2Cl_2/petroleum ether = 7/3) (Scheme 1).

In order to increase the BODIPYs singlet-to-triplet state crossing, thereby enhancing singlet oxygen production rate, compounds **3** and **4** were obtained by the insertion of iodine atoms at the 2,6-positions of compounds **3a** and **4a** (Scheme 1). This feature is known as "heavy atom effect".[19,22,23] Regarding the iodination process, we found that the reaction conditions reported in the literature[7] led to low yields of the desired compound. Therefore, we used milder conditions (treatment with iodine and iodic acid at 20–25 °C for 24 h) to allow increased yields (above 55%) in this crucial step.[24]

2.2. Chemico-physical properties

BODIPYs **3** and **4** were isolated as pure compounds as confirmed by NMR analysis UV–vis absorption spectra and HPLC retention time (Rt). The comparison of the data obtained for **3** and **4** with those of the non-iodinated precursors (**3a** and **4a**), allowed an easier determination of the structure.

In agreement with results previously published by our group on other BODIPYs, the iodination process caused a bathochromic shift of about 30 nm (Table 1), leading to a better overlapping with the emission profile of the green LED source used in biological and photobleaching experiments.[24] Moreover, the batochromic effect was associated with a more than 45% hyperchromic effect, as evidenced by the ε values. This effect can further improve the PS efficiency: as a matter of fact, higher absorbances correspond to higher extinction coefficients (i.e. more energy). In this manner, a high energy absorption should allow the use of lower PS doses to obtain a significant cell death upon activation, thus limiting undesirable side effects that may occur when an excessive PS dosage needs to be used to get an efficient photodynamic effect.[25]

Fluorescence data, reported in Table 1, were normalized to the value obtained using fluorescein as standard. As expected, the values show that the introduction of two iodine atoms on the BODIPYs **3** and **4** induced a strong decrease in the quantum yield of fluorescence; actually, the two heavy atoms exerted the known intersystem crossing (ISC) effect, thus shifting the excited state of singlet to a lower energy triplet state. This event prompts a nearly complete inhibition of fluorescence in favor of a very high rate of singlet oxygen generation.

As far as LogP values are concerned, it is well known that high values cannot be determined following spectroscopic analyses of both octanol and aqueous phases as high-lipophilic compounds do not sufficiently distribute in the aqueous phase.[26] However, computational models are available to calculate LogP values from the molecular structure of the studied compounds.[27,28] In this study, LogP values have been calculated from SMILES (Simplified Molecular Input Line Entry System) strings, which encode for the molecular structure of the four BODIPYs listed in Table 2.

To confirm these empirical data, the evaluation of a relative scale of lipophilicity of chemical compounds, belonging to a homogeneous series, has been performed measuring HPLC retention time (Rt) on a reversed phase (C18) column. Under standardized conditions (i.e. fixed eluant composition and constant flux), the most lipophilic compound usually shows the highest Rt.[26]

SMILES strings, calculated LogP values and correlations with HPLC Rt expressed in seconds are reported in Table 2 and Table 3.

Results show that, as expected, the ranking obtained in HPLC on the basis of retention time is the same as the ranking based on lipophilicity suggested by the calculated LogP (i.e. lipophilicity increases with the number of atoms and the presence of iodine atoms in the following order C4 **3a** < C4 **3** < C8 **4a** < C8 **4)**. These results are further supported by large correlations reported in Table 3 which show the consistency of LogP calculations using different computational approaches and software, compared with HPLC Rt. For this reason, the average of Crippen LogP and Galas LogP values can be considered as a fair indicator of the lipophilicity of the four BODIPYs.

Therefore, as mentioned above, BODIPYs with the four carbon

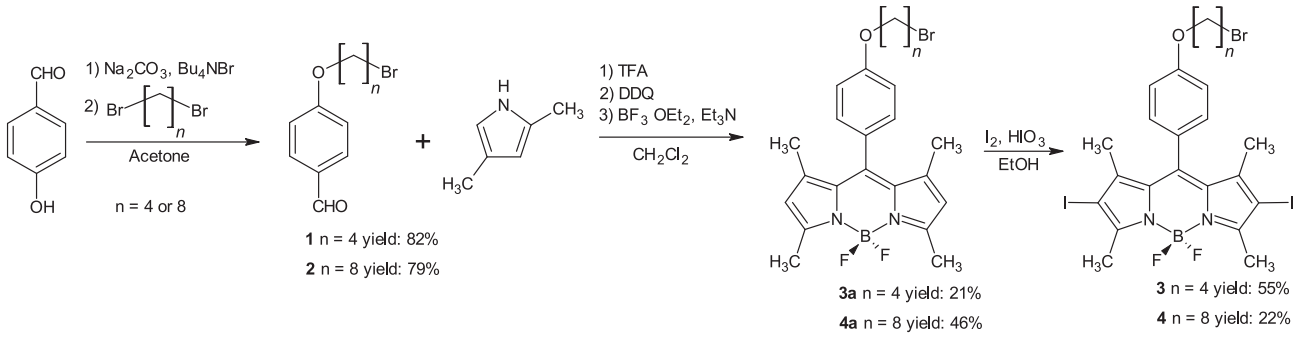

Scheme 1. Synthetic approach to obtain the iodinated BODIPYs **3** and **4**.

Table 1
Wavelength of maximum absorption and extinction coefficient, wavelength of emission, fluorescent quantum yield and singlet oxygen production for BODIPYs **3a**, **3**, **4a** and **4**.

Appendix	PS	λ_{max}[1] (nm)	ε[1] (M^{-1} cm^{-1})	λ_{em}[1] (nm)	Φ_{fluo}[2]	$^1O_2$ production[3,4]
C4	**3a**	503	44,100	542	0.66	n.d.
	3	533	66,072	552	0.01	1.10
C8	**4a**	501	28,200	541	0.52	n.d.
	4	534	41,500	554	0.01	1.11

[1] DCM was used as solvent.
[2] Φ quantum efficiency of fluorescence with fluorescein (0.1 M NaOH, 0.85) as reference.
[3] Data were normalized vs the decay rate of DPBF in the presence of Rose Bengal.
[4] Determined in isopropanol.

atoms appendix (**3a** and **3**) proved to be less lipophilic than BODIPYs with the eight carbon atoms appendix (**4a** and **4**). Moreover, the presence of voluminous and low polar iodine atoms confers a higher lipophilicity to iodinated BODIPYs compared to the non-iodinated compounds.

The relative rates of singlet oxygen ($^1O_2$) produced by the BODIPYs (25 μM) were experimentally measured by monitoring the disappearance of the 410 nm absorbance band of the 1,3-diphenylisobenzofuran (DPBF) in isopropanol and normalized to the value obtained using Rose Bengal, a well-known excellent $^1O_2$ producer, as standard. The results, reported in Table 1, indicate that **3** and **4** were able to produce high levels of singlet oxygen and these levels were comparable to that produced by Rose Bengal.

The decrease in BODIPYs absorbance intensity during 2 h irradiation with green LED light was evaluated to determine the photostability percentages of **3** and **4** along with the possible appearance of modified absorbance profiles, indicating the formation of different species.

The results obtained show that both compounds retained approximately 40% of the initial absorbance following 2 h irradiation (Fig. 1); moreover, titration curves indicate that the decay occurred faster during the first hour than the second hour, suggesting second-order decay kinetics. No modifications of the absorbance profile were observed for both BODIPY (data not shown). This last result excludes the possibility that different photoactive species could be formed through the photobleaching process.[29]

Table 3
Correlation matrix among calculated LogP values and HPLC Rt reported in Table 2.

	PADEL Crippen LogP	ACD Galas LogP	HPLC Rt (RP-C18) seconds
PADEL Crippen LogP	1		
ACD Galas LogP	0.992	1	
HPLC Rt (RP-C18) Seconds	0.997	0.997	1

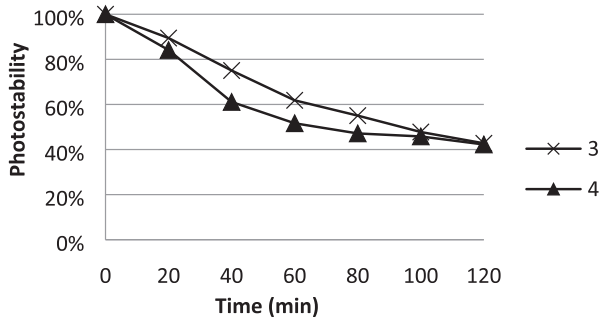

Fig. 1. Photostability of the BODIPYs during irradiation with green LED light.

2.3. Photodynamic effects in cancer cell lines

The effects of **3** and **4** on HCT116, SKOV3 and MCF7 cell viability, following 24 h treatment with the BODIPYs, 2 h irradiation with green LED light and 24 h incubation in drug-free medium in the dark are reported in Fig. 2, which shows the dose–response curves obtained according to the MTT assays. The intrinsic cytotoxicity of BODIPYs was assessed by omitting the irradiation step from the treatment protocol and it was found negligible in all cases up to concentrations tenfold higher than those used for PDT experiments (data not shown). Thus, as a whole these results confirm that irradiation is an essential requirement to activate the cytotoxic activity of these compounds.

Table 2
SMILES strings, Crippen LogP and Galas LogP (using PaDEL-Descriptor and ACD/LogP software respectively) and their average (Av. LogP), as well as HPLC Retention time expressed in seconds for the four BODIPYs (**3a**, **3**, **4a**, **4**).

Appendix	PS	SMILES	PADEL Crippen LogP	ACD Galas LogP	Av. LogP	HPLC Rt (RP-C18) seconds
C4	**3a**	BrCCCCOc1ccc(cc1)C = 1c2c(C)cc(C)n2[B-](F)(F)[N +]2 = C(C)C=C(C)C2 = 1	5.59	4.51	5.05	643
	3	BrCCCCOc1ccc(cc1)C1 = C2C(C) = C(I)C(C) = [N +]2[B-](F)(F)n2c1c(C)c(I)c2C	6.96	5.35	6.15	856
C8	**4a**	BrCCCCCCCCOc1ccc(cc1)C = 1c2c(C)cc(C)n2[B-](F)(F)[N +]2 = C(C)C=C(C)C2 = 1	7.15	5.51	6.33	868
	4	BrCCCCCCCCOc1ccc(cc1)C1 = C2C(C) = C(I)C(C) = [N +]2[B-](F)(F)n2c1c(C)c(I)c2C	8.52	6.77	7.64	1125

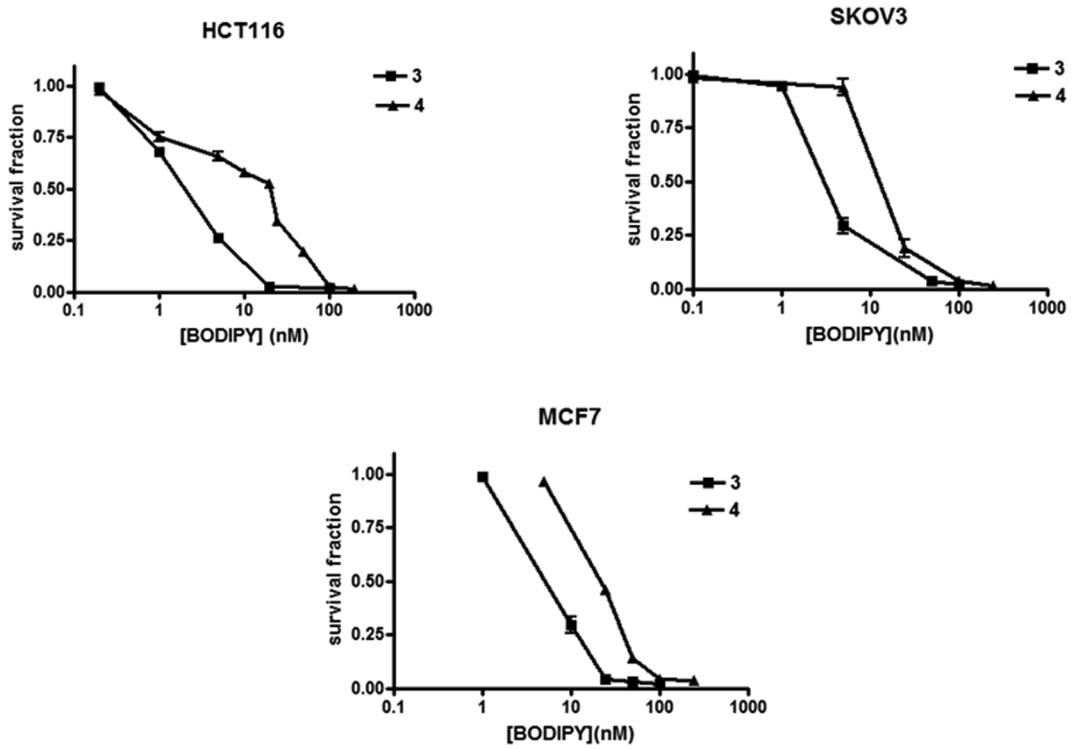

Fig. 2. Dose-response curves obtained in HCT116, SKOV3 and MCF7 cell lines by the MTT assay, following 24 h treatment with **3** and **4**, 2 h irradiation, 24 h incubation in drug-free medium (mean ± S.E.M. of 3–5 independent experiments).

Table 4
IC_{50} (nM) values obtained in HCT116, SKOV3 and MCF7 cells following treatment with **3** and **4** for 24 h, 2 h irradiation, 2 h incubation in drug-free medium and subsequent MTT test. (mean ± S.E.M. of 3–5 independent experiments).

	HCT116	SKOV3	MCF7
3	2.0 ± 0.09 [a]	3.56 ± 0.28[c]	6.88 ± 0.66 [e]
4	11.7 ± 0.84[b]	15.61 ± 1.34 [d]	23.11 ± 0.87

[a] $p < 0.001$ vs MCF7 same compound and $p < 0.001$ vs **4** same cell line.
[b] $p < 0.001$ vs MCF7 same compound.
[c] $p < 0.05$ vs MCF7 same compound and $p < 0.001$ vs **4** same cell line.
[d] $p < 0.001$ vs MCF7 same compound; e $p < 0.001$ vs **4** same cell line.

The IC_{50} values reported in Table 4 show that the two BODIPYs affected HCT116, SKOV3 and MCF7 viability at submicromolar concentrations; interestingly, **3** was significantly more potent than **4** in all cell lines. As already reported for other BODIPYs, differences in potency can correlate to lipophilicity and to molar extinction coefficient of the compounds;30] thus, the lower lipophilicity and even the higher molar extinction coefficient observed for **3,** compared to **4** (LogP and ε, respectively), may account for its greater photodynamic activity.

Interestingly, MCF7 cells were significantly more resistant to **3** and **4** than HCT116 and SKOV3 cell lines. Some authors reported that the final response to PDT could be influenced by both the tumor suppressor p53 and p53-related proteins.[31–33] In particular, wt p53 seems to play an important role in triggering efficient apoptosis in cells following PDT.31 However, the role of p53 status in the response of cancer cell lines to PDT is still controversial and conflicting responses to PDT have also been observed in cells with p53 wt.[34,35] In agreement with this disputed situation, HCT116 and MCF7 cells, both expressing wt p53, showed a very different response to the studied BODIPYs. Maybe the resistance to **3** and **4** observed in MCF7 cells could be the result of a different expression of p53-related proteins or other p53 family members, but this was not specifically addressed in this work.

Flow cytometric analysis of BODIPYs-treated cells did not show a significant arrest in G1 phase, indicating that both the PS does not affect entry in the cell cycle (Fig. 3) and suggesting that the effect of the compounds is not generically cytostatic. Cell cycle analysis performed by omitting the irradiation step were similar to those obtained in photoactiveted cells (data not shown). Therefore, the two BODIPYs do not seem to have any significant effect on cell cycle distribution, both in the presence and in the absence of photoactivation.

Apoptotic cell death appears to play a central role in tumor cell death induced by the two BODIPYs, in agreement to what we and other authors have described for a number of photosensitizers.[30,36–38] More specifically, 24 h exposure to equitoxic concentrations of **3** and **4** (corresponding to the respective IC_{50} values reported in Table 4), 2 h irradiation and 24 h incubation in PS-free medium were able to induce a significant increase in the percentage of apoptotic cells over control in HCT116, SKOV3 and MCF7 cells (Fig. 4 A). Furthermore, necrotic cell death seemed to contribute to the photodynamic killing effect of these BODIPYs in SKOV3 and MCF7 cell lines, as indicate the significant increase of the percentage of necrotic cells observed in these cell lines following PDT with **3** and **4** (Fig. 4 B), whereas no necrotic cell death was observed in HCT116 cells under the same experimental conditions.

When the irradiation step was omitted, none of the BODIPYs was able to trigger an apoptotic or necrotic response in any of the cell lines (data not shown).

The activation of cell death program in PDT has been reported to correlate with cellular uptake of photosensitizers.[21,30,39] Therefore, we performed a spectrophotometric analysis of BODIPYs uptake in HCT116, SKOV3 and MCF7 cells following 24 h exposition to a high concentration of **3** and **4** (10 μM). The three cell lines considered displayed different extent of intracellular accumulation of the BODIPYs (Fig. 5); however, only in MCF7 cells the amount of PS which enter the cells seems to be directly related to the observed higher cytotoxic effect of **3** with respect to **4**.

In PDT, singlet oxygen and ROS are the effectors of tumor cells death and light is used to elicit the photosensitizer to induce their

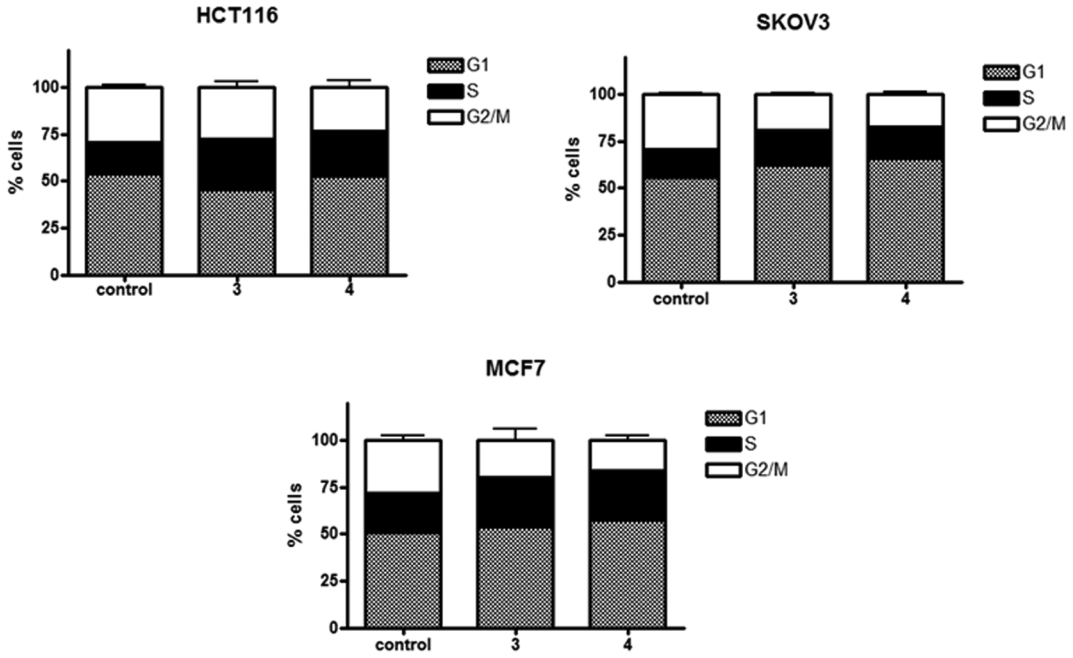

Fig. 3. Cell cycle analysis of HCT116, SKOV3 and MCF7 cell lines, following 24 h treatment with equitoxic concentrations of **3** and **4** corresponding to the IC_{50} values reported in table IV, 2 h irradiation, 24 h incubation in drug-free medium. Propidium iodide (PI) was used as fluorescent probe (mean ± S.E. of 3 independent experiments).

production.[40,41] As reported above, both **3** and **4** were as good as Rose Bengal in producing high levels of singlet oxygen. ROS production measured by flow cytometric analysis of the fluorescein fluorescence following treatment with equitoxic concentration of the BODIPYs, corresponding to their IC_{50} values reported in Table 4, indicate that **3** and **4** induced a significant increase in ROS levels over control in SKOV3 cells; specifically, in this cell line **3** was more effective than **4** in generating ROS (Fig. 6). On the contrary, no significant increase in ROS production was observed in HCT116 and MCF7 cells or when flow cytometry was performed 24 h later (data not shown), indicating that both ROS generation and persistence abate within 24 h from the end of irradiation. These results suggest that **3** and **4** exert their photodynamic activity on HCT116 and MCF7 cells preferentially through type II reaction (singlet oxygen production) while type I and type II (ROS production) reactions occurred simultaneously in SKOV3 cells.

Tumor cells of epithelial origin may possess intrinsic migratory behavior, that has been reported as a mark of invasion and metastasis, indicating that the cells have undergone an epithelial-to-mesenchimal transition.[38,42] A number of PSs, such as a Photofrin derivative, have shown anti-migratory activity.[38,43,44] However, no data concerning the anti-migratory activity of BODIPY have been reported to date, thus, we decided to evaluate the effect of **3** and **4** on cellular migration using the scratch wound healing assay. Between the cell lines included in this study, only SKOV3 cells were able to spontaneously migrate and as a matter of fact their higher motility correlates with a higher degree of malignancy, as compared to HCT116 and MCF7 cells.

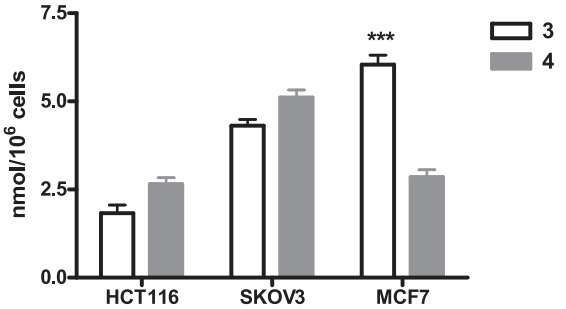

Fig. 5. Uptake of **3** and **4** in HCT116, SKOV3 and MCF7 cells following 24 h exposition to the BODIPYs (10 μM) (mean ± S.E. of 3–5 independent experiments; ***p < 0.001 vs **4** same cell line).

The results showed in Fig. 7 indicate that, following photoactivation, subtoxic concentrations of **3** and **4** were able to slow down the intrinsic migratory capacity of SKOV3 cells, albeit to varying degrees; in the absence of irradiation none of the compounds were able to interfere with the intrinsic migratory activity of SKOV3 cells (data not shown).

Analysis of the percentage of open scratch, performed using the

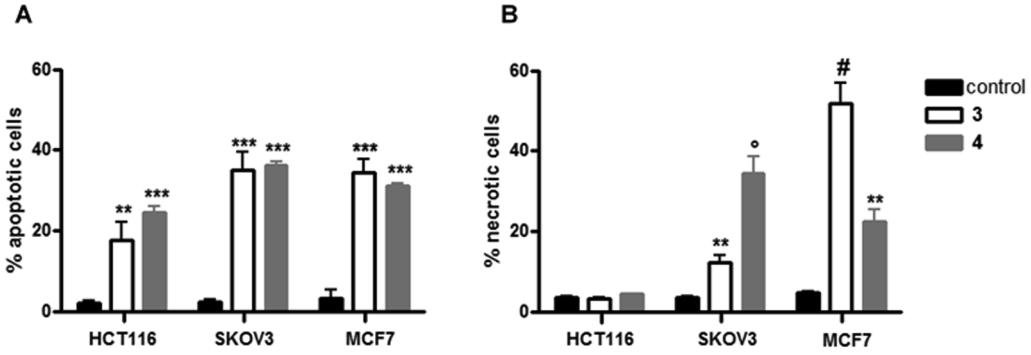

Fig. 4. Percentage of apoptotic (A) and necrotic (B) HCT116, SKOV3 and MCF7 cells following PDT with equitoxic concentrations of **3** and **4**, corresponding to the IC_{50} values (mean ± S.E. of 3–5 independent experiments). **p < 0.01 vs control same cell line; ***p < 0.001 vs control same cell line; °p < 0.001 vs control and **3** same cell line; #p < 0.001 vs control and **4** same cell line.

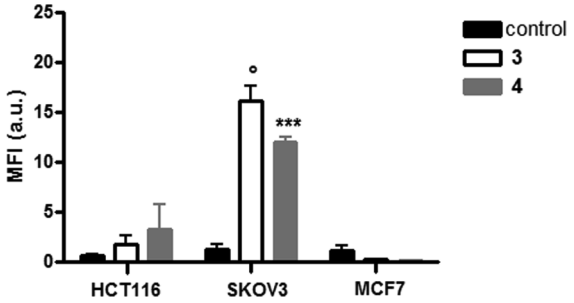

Fig. 6. ROS generation in HCT116, SKOV3 and MCF7 cells following 24 h exposure or not (control) to **3** and **4** at their respective IC_{50} values and 2 h irradiation in compounds-free PBS. The intracellular ROS levels were determined by flow cytometry at the end of the irradiation period. Mean ± S.E.M. of three independent experiments. *** $p < 0.001$ vs controls and $p < 0.05$ vs **4**, ** $p < 0.001$ vs controls.

TScratch software, indicate that the antimigratory effect of **3** was significantly higher than **4** (Table 5).

3. Conclusions

Taken together, these data indicate that the presence of an appendix consisting of linear carbon atoms chain of different length on the phenyl group placed on the position 8 of the dipyrrolylmethene basic structure give the two BODIPYs a different degree of lipophilicity, resulting in a significant more efficient phototoxic effect of the molecule with lower lipophilicity (i.e. **3**). Thus, due to its high lipophilicity, compound **4** could probably form aggregates in the aqueous medium used for photodynamic experiments, leading to a less effective photodynamic activity.

Table 5
Percentage of open scratch wound in SKOV3 cells following 24 h treatment with **3** (0.75 nM) and **4** (2.5 nM), 2 h irradiation under green LED light and 24 h incubation in drug-free medium at 37 °C. Pictures of the scratch wound were taken immediately following the irradiation step (0) and after 24 h; percentage of open scratch wound were evaluated by the TScratch software (mean ± S.E.M. of 3 independent experiments).

	0	24 h
Control	38.27 ± 3.02	8.68 ± 0.58[a]
3	35.19 ± 2.61	24.81 ± 2.54[b]
4	37.71 ± 0.78	13.53 ± 0.14[c]

[a] $p < 0.001$ vs 0 same treatment.
[b] $p < 0.05$ vs 0 same treatment and $p < 0.01$ vs control and **4** 24 h.
[c] $p < 0.001$ vs 0 same treatment and $p < 0.05$ vs control 24 h.

Furthermore, as supported by previously reported data, the presence of the bromine atom at the end of the alkyl chain could offer a great synthetic ductility, allowing subsequent nucleophilic substitution reactions either to introduce positive charges or to hook, through a covalent bond, the BODIPY on nanoparticles for a more efficient drug delivery.[21]

Apoptotic and necrotic cell deaths appear to play a pivotal role in tumor cell death induced by the two BODIPYs, mediated by a singlet oxygen and ROS level increase. Further investigations are required to clearly explain the molecular mechanisms underlying the better response observed with **3**, compared with **4**. However, the present data suggest the potential use of **3** for PDT, also considering the interesting results concerning the anti-migratory effect of this BODIPY.

A potential problem concerning the application of these BODIPYs

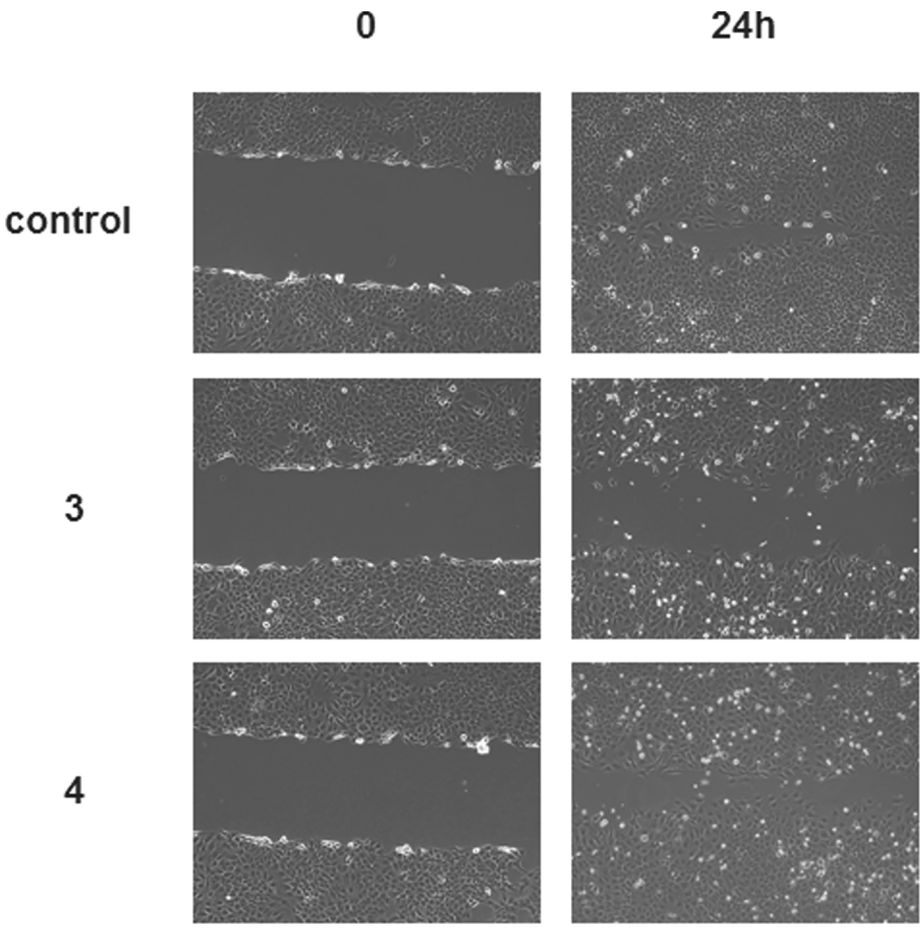

Fig. 7. Migratory activity of SKOV3 cells following treatment with **3** (0.75 nM) and **4** (2.5 nM)for 24 h, scratch formation, 2 h irradiation and incubation for 24 h in drug-free medium at 37 °C. Pictures of the scratch wound were taken immediately following the irradiation step (0) and after 24 h, through a camera connected to an Olympus IX81 microscope.

for PDT, especially in tumors which are not superficial, is that absorption in the red region of the visible spectrum is required for clinical applications, due to the ability of red light to penetrate deeper into the tumor, whereas their optimal absorption wavelength lies in the green region. However, the activation by green light can be useful when superficial treatment is required and more penetrating wavelengths could present a threat to contiguous organs.[45] In addition, it has been reported that a red-shift in the λ_{max} could be easily gained by introducing two styryl substituents in the α position of the BODIPY, thus obtaining compounds featuring optimal absorption at approximately 650 nm, which makes those particularly attractive in view of their possible use as PSs for photodynamic cancer therapies.[46] Finally, the emergence of new technologies for photodynamic activation and light or PS delivery is going to redefine the traditional views that PDT is limited to superficial tumors.[47] Moreover, in the long term, the availability of radiosensitizers, biocompatible nanoparticles, upconverting nanomaterials and the ability to design personalized light delivery protocols could make PDT a viable therapy that has significant impact in deep tissues and enhances overall outcomes.

4. Materials and methods

4.1. Chemical

UV–vis absorption spectra, ^{1}H NMR spectra, mass spectrometric measurements, HPLC analyses were performed as previously reported.[48] Merck 60 F254 silica gel precoated sheets (0.2 mm thick) were used for analytical thin-layer chromatography (TLC). Silica gel 60 (70–230 mesh, Merck) was used for column chromatographic separations. 4-hydroxybenzaldehyde, 1,4-dibromobutane, 1,8-dibromooctane and 2,4-dimethylpyrrole were used as received by the supplier (Sigma-Aldrich). Dichloromethane (CH_2Cl_2), used in the synthesis of BODIPYs, was freshly distilled directly into the reaction flask.

The green LED array is composed of 12 × 3 W diodes placed on a 11 cm diameter disk and equipped with a heat sinker. The emitted light is characterized by lambda max (λ_{max}) of emission at 525 nm and width at half maximum of 70 nm (fluence rate 3.036 × 10^{-3} W/cm^2; light energy density, or fluence, 21.8 J/cm^2). A 50 W current transformer provided electric supply. The LED array was placed above the samples at such a distance as to produce a homogeneous area of irradiation.

4.1.1. Synthesis of 4-[(4-bromobutyl)oxy]benzaldehyde (1) and of 4-[8-bromooctyl)oxy]benzaldehyde (2)

4-[(4-bromobutyl)oxy]benzaldehyde (**1**) and 4-[8-bromooctyl)oxy] benzaldehyde (**2**) were synthetized accordingly to the methods reported by Caruso et al.[38]

4.1.1.1. Synthesis of 2,6-diiodo-1,3,5,7-tetramethyl-8-{4-[(4-bromobutyl) oxy]phenyl}-4,4′-difluoroboradiazaindacene (3).

4-[(4-bromobutyl)oxy] benzaldehyde and (838 mg, 3.2 mmol) and 2,4-dimethylpyrrole (724 μL, 7.04 mmol) were dissolved in dry CH_2Cl_2 (60 mL) under N_2 atmosphere; then twenty drops of TFA were added and the solution was stirred at RT overnight until the complete consumption of the aldehyde, as determined by TLC analysis (SiO_2, CH_2Cl_2). Thereafter the dipyrrolylmethane to dipyrrolylmethene oxidation was achieved by adding solid DDQ (1.09 g, 4.8 mmol) and stirring the mixture for 2 h. The last step of the BODIPY synthesis requires the addition of Et_3N (5 mL) and $BF_3{\cdot}OEt_2$ (5 mL) to the reaction mixture. After 24 h under stirring, the organic layer was washed two times with water, one time with 1 M HCl solution and two more times with water; the organic solution was then dried over Na_2SO_4, filtered, and evaporated to dryness. The raw material was purified by column chromatography (SiO_2, CH_2Cl_2/petroleum ether = 7/3) affording 317 mg (0.668 mmol, yield: 20.9%) of the desired compound (**3a**) as orange needles. $C_{23}H_{26}BBrF_2N_2O$ MW = 475.18; UV–Vis (DCM): 503 nm (ε = 44100); ^{1}H NMR ($CDCl_3$) δ: 1.46 (s, 6H, 2 × CH_3); 2.03 (m, 2H, CH_2); 2.13 (m, 2H, CH_2); 2.58 (s, 6H, 2 × CH_3); 3.55 (t, 2H, CH_2Br); 4.08 (t, 2H, CH_2O); 6.00 (s, 2H, 2 × CH_2); 7.02 (d, 2H, 2 × CH); 7.19 (d, 2H, 2 × CH); HPLC retention time: 10′34″ (100%).

The corresponding 2,6-diiodo compound (**3**) was obtained by adding 431 mg of I_2 (1.545 mmol) and 299 mg of HIO_3 (1.545 mmol) to an ethanol solution of **3a** (317 mg, 0.668 mmol). This mixture was stirred for 24 h at RT, washed with water and extracted three times with CH_2Cl_2; the organic phase was dried over Na_2SO_4 and evaporated to dryness. The crude product was purified by column chromatography (SiO_2, CH_2Cl_2/petroleum ether = 1/1) affording 266 mg (0.37 mmol; yield: 54.80%) of 14 as red needles.

Compound **3**: $C_{23}H_{24}BBrF_2I_2N_2O$ M.W.: 726.97 g/mol; UV–Vis (DCM): 533 nm (ε = 66072); ^{1}H NMR ($CDCl_3$) δ: 1.47 (s, 6H, 2 × CH_3); 2.04 (m, 2H, CH_2); 2.16 (m, 2H, CH_2); 2.62 (s, 6H, 2 × CH_3); 3.54 (t, 2H, CH_2Br); 4.09 (t, 2H, CH_2O); 7.04 (d, 2H, 2 × CH); 7.15 (d, 2H, 2 × CH); MS (ESI): $M-1^+$ found: 726.01 calcd for $C_{23}H_{24}BBrF_2I_2N_2O$ 726.97; HPLC retention time: 14′16″ (100%).

4.1.2. Synthesis of 2,6-diiodo-1,3,5,7-tetramethyl-8-{4-[(8-bromooctyl) oxy]phenyl}-4,4′-difluoroboradiazaindacene (4)

1,3,5,7-tetramethyl-8-{4-[(8-bromooctyl)oxy]phenyl}-4,4′-difluoroboradiazaindacene (**4a**) and 2,6-diiodo-1,3,5,7-tetramethyl-8-{4-[(8-bromooctyl)oxy]phenyl}-4,4′-difluoroboradiazaindacene (**4**) were synthetized accordingly to the methods reported by Zagami et al.[49]

4.1.3. Comparative Singlet-Oxygen generation measurements

The ability of the two BODIPYs to generate $^1O_2$ was measured by monitoring the disappearance of the 410 nm absorbance band of DPBF, a known $^1O_2$ scavenger and the relative singlet oxygen generation rates for **3** and **4** were determined by comparison to the rate obtained with Rose Bengal as previously reported.[24]

4.1.4. LogP determination

The hydrophobicity was estimated using the software PaDEL-Descriptor[27] and ACD Labs[28] calculated LogP values i.e. Crippen LogP[50] and Galas LogP.[28] Structural Description of the two BODIPYs (compounds **3** and **4**) and of their precursors (compounds **3a** and **4a**) was encoded into SMILES strings which were used as input for the LogP calculations. SMILES strings and calculated values are listed in Table 2.

4.1.5. Photostability

The stability of BODIPYs **3** and **4** was evaluated using a UV-vis spectrophotometer, by measuring every 20 min the decrease of the absorbance profile of 10 μM solutions during 2 h irradiation with green LED light. The decrease in the absorbance intensity al the lambda max (530 nm) vs time plot was used to determine the photostability percentage.

4.1.6. Fluorescence properties and quantum yield of fluorescence

The fluorescence properties of the BODIPYs were studied as previously reported.[48]

4.2. Biological

4.2.1. Cell lines and photodynamic studies

The human colon carcinoma HCT116 and the ovarian cancer SKOV3 cell lines were maintained in Dulbecco's Modified Eagle Medium (DMEM, Sigma-Aldrich), while the human breast cancer MCF7 cells were cultured in Roswell Park Memorial Institute 1640 (RPMI1640, Sigma-Aldrich) medium, supplemented with 10% fetal bovine serum, 1% glutamine, 0.25% neomycin and 0.5% penicillin–streptomycin (Sigma-Aldrich). All the cell lines were maintained in standard culture conditions at 37 °C in a humidified 5% CO_2 atmosphere.

The effects of the BODIPYs on HCT116, SKOV3 and MCF7 cell viability were evaluated by performing the MTT assay as previously described.[38,51,52] Briefly, cells seeded in 96-well plates could attach for

24 h prior the exposition to the BODIPYs (0.1 and 200 nM) at 37 °C. After 24 h, the drug-containing medium was replaced by fresh PBS, and cells were irradiated using a green LED source for 2 h. Cells were then incubated in the dark at 37 °C in drug-free medium for 24 h and following 3 h incubation in the presence of MTT (2 mg/mL in PBS) absorbance of DMSO-dissolved formazan crystals was measured at 595 nm using Infinite® 200 PRO (Tecan). Possible intrinsic (i.e. not photoinduced) effects of the BODIPYs were assessed by omitting the irradiation step in cells treated with concentrations of BODIPY tenfold higher (1–2000 nM) than those used for irradiated cells.

IC_{50} values were estimated from concentration-response curves by non-linear regression analysis, using GraphPad Prism software, v. 5.0 (GraphPad, San Diego, CA, USA).

4.2.2. Flow cytometric analysis

The ability of the tested BODIPY to induce apoptotic and/or necrotic cell death and/or alterations in the distribution of DNA through the cell cycle was evaluated, following 24 h exposition to **3** and **4** at their respective IC_{50} (the values are reported in Table 4), 2 h irradiation in drug-free PBS and 24 h incubation in drug-free medium in the dark, by flow cytometric analysis as previously reported.[38]

Intracellular ROS levels were evaluated using 2,7-dichlorodihydrofluoresceindiacetate (DCFH-DA) as a probe. Cells were processed and analyzed at the end of the irradiation period.[38]

All the samples were analyzed with a FACSCalibur flow cytometer (Becton Dickinson Mountain View, CA, USA) and data were processed using CellQuest software (Becton Dickinson). PI and fluorescein fluorescence were collected through a 575 nm and 530 nm band-pass filter, respectively. The percentage of apoptotic cells was determined based on the sub-G1 peaks detected in monoparametric histograms acquired in log mode, while the DNA distribution through the different phases of cell cycle was determined on peaks acquired in linear mode. Finally, intracellular ROS generation was quantitated in arbitrary units based on the mean fluorescence intensity (MFI). For all the cytometric analysis, in control samples the treatment with the two BODIPY was omitted.

4.2.3. Cellular uptake

3×10^6 cells were seeded onto 75 cm^3 flask and allowed to grow for 48 h prior to treatment with BODIPYs at the concentration of 10 μM. After 24 h, cells were harvested by trypsinization and lysed with NaOH 0.1 M solution containing SDS 1% (5×10^6 cells/mL). The absorbance of each BODIPY was measured at the λ_{max}. The BODIPY concentrations in the samples were extrapolated from a calibration curve, obtained by measuring the absorbance values of known concentrations of PSs in SDS-lysed cells solution.

4.2.4. Effects on cellular migration

Preliminary experiments have shown that only SKOV3 out of the three cell lines tested exhibited intrinsic migratory properties, therefore the effect of **3** and **4** on cell migration was evaluated on this cell line by the scratch wound healing assay. Briefly, 7×10^5 cells/well were grown for 48 h (approximately to confluence) in 6-well plates before 24 h treatment with subtoxic concentration of **3** (0.75 nM) and **4** (2.5 nM). A scratch in cell monolayers was then performed using 1-mL pipette tip and following replacement of drug-containing medium by fresh PBS, cells were irradiated under green LED light for 2 h and incubated for 24 h in drug-free medium at 37 °C. Pictures of the scratch wound were taken immediately following the irradiation step (0) and after 24 h, through a camera connected to an Olympus IX81 microscope. Percentage of open scratch wound were evaluated by the TScratch software.

4.2.5. Statistical analysis

Differences between IC_{50} values, percentage of apoptotic or necrotic cells, intracellular ROS levels, BODIPYs uptake and percentage of open scratch wounds were evaluated statistically by analysis of the variance with Bonferroni post-test for multiple comparisons.

Funding

This study was supported by the Università degli Studi dell'Insubria, Fondi di Ateneo per la Ricerca "FAR2018" and "FAR2019" (to MBG and EC). The funding agencies were not involved in the research plan and the interpretation of the data.

Declaration of Competing Interest

The authors declare that they have no known competing financial interests or personal relationships that could have appeared to influence the work reported in this paper.

References

1. Baptista MS, et al. Type I and Type II photosensitized oxidation reactions: guidelines and mechanistic pathways. *Photochem Photobiol.* 2017;93:912–919. https://doi.org/10.1111/php.12716.
2. Dolmans DEJGJ, Fukumura D, Jain RK. Photodynamic therapy for cancer. *Nat Rev Cancer.* 2003;3:380–387. https://doi.org/10.1038/nrc1071.
3. Lan M, Zhao S, Liu W, Lee C-S, Zhang W, Wang P. Photosensitizers for photodynamic therapy. *Adv Healthc Mater.* 2019;8. https://doi.org/10.1002/adhm.201900132.
4. O'Connor AE, Gallagher WM, Byrne AT. Porphyrin and nonporphyrin photosensitizers in oncology: Preclinical and clinical advances in photodynamic therapy. *Photochem Photobiol.* 2009;85:1053–1074. https://doi.org/10.1111/j.1751-1097.2009.00585.x.
5. Abrahamse H, Hamblin MR. New photosensitizers for photodynamic therapy. *Biochem J.* 2016;473:347–364. https://doi.org/10.1042/BJ20150942.
6. Kamkaew A, Lim SH, Lee HB, Kiew LV, Chung LY, Burgess K. BODIPY dyes in photodynamic therapy. *Chem Soc Rev.* 2013;42:77–88. https://doi.org/10.1039/c2cs35216h.
7. Lim SH, et al. In vitro and in vivo photocytotoxicity of boron dipyrromethene derivatives for photodynamic therapy. *J Med Chem.* 2010;53:2865–2874. https://doi.org/10.1021/jm901823u.
8. Liu J-Y, Zhou P-Z, Ma J-L, Jia X. Trifluoromethyl boron dipyrromethene derivatives as potential photosensitizers for photodynamic therapy. *Molecules.* 2018;23. https://doi.org/10.3390/molecules23020458.
9. Atilgan S, Ekmekci Z, Dogan AL, Guc D, Akkaya EU. Water soluble distyryl-boradiazaindacenes as efficient photosensitizers for photodynamic therapy. *Chem Commun.* 2006;42:4398–4400. https://doi.org/10.1039/b612347c.
10. Ziessel R, Ulrich G, Harriman A. The chemistry of Bodipy: A new El Dorado for fluorescence tools. *New J Chem.* 2007;31:496–501. https://doi.org/10.1039/b617972j.
11. Erten-Ela S, Yilmaz MD, Icli B, Dede Y, Icli S, Akkaya EU. A panchromatic boradiazaindacene (BODIPY) sensitizer for dye-sensitized solar cells. *Org Lett.* 2008;10:3299–3302. https://doi.org/10.1021/ol8010612.
12. Singh-Rachford TN, Haefele A, Ziessel R, Castellano FN. Boron dipyrromethene chromophores: Next generation triplet acceptors/annihilators for low power upconversion schemes. *J Am Chem Soc.* 2008;130:16164–16165. https://doi.org/10.1021/ja807056a.
13. Karolin J, Johansson LBA, Strandberg L, Ny T. Fluorescence and absorption spectroscopic properties of dipyrromethene boron difluoride (BODIPY) derivatives in liquids, lipid membranes, and proteins. *J Am Chem Soc.* 1994;116:7801–7806. https://doi.org/10.1021/ja00096a042.
14. Wittmershaus BP, Skibicki JJ, McLafferty JB, Zhang Y-Z, Swan S. Spectral properties of single BODIPY dyes in polystyrene microspheres and in solutions. *J Fluoresc.* 2001;11:119–128. https://doi.org/10.1023/A:1016629518660.
15. Dost Z, Atilgan S, Akkaya EU. Distyryl-boradiazaindacenes: facile synthesis of novel near IR emitting fluorophores. *Tetrahedron.* 2006;62:8484–8488. https://doi.org/10.1016/j.tet.2006.06.082.
16. Liu J-Y, Yeung H-S, Xu W, Li X, Ng DKP. Highly efficient energy transfer in subphthalocyanine - BODIPY conjugates. *Org Lett.* 2008;10:5421–5424. https://doi.org/10.1021/ol8023677.
17. Kue CS, et al. Recent strategies to improve boron dipyrromethene (BODIPY) for photodynamic cancer therapy: An updated review. *Photochem Photobiol Sci.* 2018;17:1691–1708. https://doi.org/10.1039/c8 pp00113h.
18. Banfi S, Caruso E, Zaza S, Mancini M, Gariboldi MB, Monti E. Synthesis and photodynamic activity of a panel of BODIPY dyes. *J Photochem Photobiol B Biol.* 2012;114. https://doi.org/10.1016/j.jphotobiol.2012.05.010.
19. Chen K, et al. Bodipy derivatives as triplet photosensitizers and the related intersystem crossing mechanisms. *Front Chem.* 2019;7. https://doi.org/10.3389/fchem.2019.00821.
20. Boens N, Verbelen B, Ortiz MJ, Jiao L, Dehaen W. Synthesis of BODIPY dyes through postfunctionalization of the boron dipyrromethene core. *Coord Chem Rev.* 2019;399. https://doi.org/10.1016/j.ccr.2019.213024.
21. Ballestri M, et al. Core–shell poly-methyl methacrylate nanoparticles covalently functionalized with a non-symmetric porphyrin for anticancer photodynamic

therapy. *J Photochem Photobiol B Biol.* 2018;186. https://doi.org/10.1016/j.jphotobiol.2018.07.013.
22. Yogo T, Urano Y, Ishitsuka Y, Maniwa F, Nagano T. Highly efficient and photostable photosensitizer based on BODIPY chromophore. *J Am Chem Soc.* 2005;127:12162–12163. https://doi.org/10.1021/ja0528533.
23. Gorman A, Killoran J, O'Shea C, Kenna T, Gallagher WM, O'Shea DF. In vitro demonstration of the heavy-atom effect for photodynamic therapy. *J Am Chem Soc.* 2004;126:10619–10631. https://doi.org/10.1021/ja047649e.
24. Banfi S, Nasini G, Zaza S, Caruso E. Synthesis and photo-physical properties of a series of BODIPY dyes. *Tetrahedron.* 2013;69:4845–4856. https://doi.org/10.1016/j.tet.2013.04.064.
25. Ormond AB, Freeman HS. Dye sensitizers for photodynamic therapy. *Materials (Basel).* 2013;6:817–840. https://doi.org/10.3390/ma6030817.
26. Terada H. Determination of Log Poct by high-performance liquid chromatography, and its application in the study of quantitative structure-activity relationships. *Quantit Struct-Activity Relationships.* 1986;5. https://doi.org/10.1002/qsar.19860050302.
27. Yap CW. PaDEL-Descriptor: An open source software to calculate molecular descriptors and fingerprints. *J Comput Chem.* 2011;32:1466–1474.
28. acdlabs, "www.acdlabs.com/logp/ Advanced Chemistry Development, Inc., Toronto, ON, Canada".
29. Duan C, et al. Structural evidence for a two-regime photobleaching mechanism in a reversibly switchable fluorescent protein. *J Am Chem Soc.* 2013;135. https://doi.org/10.1021/ja406860e.
30. Gariboldi MB, et al. Photodynamic effects of novel 5,15-diaryl-tetrapyrrole derivatives on human colon carcinoma cells. *Bioorganic Med. Chem.* 2009;17. https://doi.org/10.1016/j.bmc.2009.01.035.
31. Zawacka-Pankau J, Krachulec J, Grulkowski I, Bielawski KP, Selivanova G. The p53-mediated cytotoxicity of photodynamic therapy of cancer: Recent advances. *Toxicol Appl Pharmacol.* 2008;232:487–497. https://doi.org/10.1016/j.taap.2008.07.012.
32. Kessel D. Subcellular targeting as a determinant of the efficacy of photodynamic therapy. *Photochem Photobiol.* 2017;93:609–612. https://doi.org/10.1111/php.12692.
33. Acedo P, Zawacka-Pankau J. p53 family members - Important messengers in cell death signaling in photodynamic therapy of cancer? *Photochem Photobiol Sci.* 2015;14:1390–1396. https://doi.org/10.1039/c5 pp00251f.
34. Fisher AMR, Ferrario A, Rucker N, Zhang S, Gomer CJ. Photodynamic therapy sensitivity is not altered in human tumor cells after abrogation of p53 function. *Cancer Res.* 1999;59.
35. Fisher AMR, Rucker N, Wong S, Gomer CJ. Differential photosensitivity in wild-type and mutant p53 human colon carcinoma cell lines. *J Photochem Photobiol B Biol.* 1998;42. https://doi.org/10.1016/S1011-1344(97)00130-9.
36. Kessel D, Oleinick NL. Cell death pathways associated with photodynamic therapy: an update. *Photochem Photobiol.* 2018;94:213–218. https://doi.org/10.1111/php.12857.
37. dos Santos AF, et al. Methylene blue photodynamic therapy induces selective and massive cell death in human breast cancer cells. *BMC Cancer.* 2017;17. https://doi.org/10.1186/s12885-017-3179-7.
38. Caruso E, Cerbara M, Malacarne MC, Marras E, Monti E, Gariboldi MB. Synthesis and photodynamic activity of novel non-symmetrical diaryl porphyrins against cancer cell lines. *J Photochem Photobiol B Biol.* 2019;195. https://doi.org/10.1016/j.jphotobiol.2019.04.010.
39. Heinemann F, Karges J, Gasser G. Critical overview of the use of Ru(II) polypyridyl complexes as photosensitizers in one-photon and two-photon photodynamic therapy. *Acc Chem Res.* 2017;50:2727–2736. https://doi.org/10.1021/acs.accounts.7b00180.
40. Kou J, Dou D, Yang L. Porphyrin photosensitizers in photodynamic therapy and its applications. *Oncotarget.* 2017;8:81591–81603. https://doi.org/10.18632/oncotarget.20189.
41. Huang Q, Ou Y-S, Tao Y, Yin H, Tu P-H. Apoptosis and autophagy induced by pyropheophorbide-α methyl ester-mediated photodynamic therapy in human osteosarcoma MG-63 cells. *Apoptosis.* 2016;21:749–760. https://doi.org/10.1007/s10495-016-1243-4.
42. Rajesh Y, Biswas A, Mandal M. Glioma progression through the prism of heat shock protein mediated extracellular matrix remodeling and epithelial to mesenchymal transition. *Exp Cell Res.* 2017;359:299–311. https://doi.org/10.1016/j.yexcr.2017.08.032.
43. Wang X, et al. Analysis of the in vivo and in vitro effects of photodynamic therapy on breast cancer by using a sensitizer, Sinoporphyrin sodium. *Theranostics.* 2015;5:772–786. https://doi.org/10.7150/thno.10853.
[44]. Gheewala T, Skwor T, Munirathinam G. Photodynamic therapy using pheophorbide and 670 nm LEDs exhibits anti-cancer effects in-vitro in androgen dependent prostate cancer. *Photodiagnosis Photodyn Ther.* 2018;21:130–137. https://doi.org/10.1016/j.pdpdt.2017.10.026.
[45]. Grosjean P, Wagnieres G, Fontolliet C, Van Den Bergh H, Monnier P. Clinical photodynamic therapy for superficial cancer in the oesophagus and the bronchi: 514 nm compared with 630 nm light irradiation after sensitization with Photofrin II. *Br J Cancer.* 1998;77:1989–1995. https://doi.org/10.1038/bjc.1998.330.
46. Saki N, Dinc T, Akkaya EU. Excimer emission and energy transfer in cofacial boradiazaindacene (BODIPY) dimers built on a xanthene scaffold. *Tetrahedron.* 2006;62:2721–2725. https://doi.org/10.1016/j.tet.2005.12.021.
47. Mallidi S, Anbil S, Bulin A-L, Obaid G, Ichikawa M, Hasan T. Beyond the barriers of light penetration: Strategies, perspectives and possibilities for photodynamic therapy. *Theranostics.* 2016;6:2458–2487. https://doi.org/10.7150/thno.16183.
48. Malacarne MC, Banfi S, Caruso E. In vitro photodynamic treatment of cancer cells induced by aza-BODIPYs. p. in press *Photochem Photobiol Sci.* 2020;in press. https://doi.org/10.1039/D0PP00026D.
49. Zagami R, et al. Tailored-BODIPY/Amphiphilic Cyclodextrin Nanoassemblies with PDT Effectiveness. *Langmuir.* 2018;34:8639–8651. https://doi.org/10.1021/acs.langmuir.8b01049.
50. Wildman GM, Crippen SA. Prediction of physicochemical parameters by atomic contributions. *J Chem Inf Comput Sci.* 1999;39:868–873.
51. Gariboldi MB, et al. The BH3-mimetic obatoclax reduces HIF-1α levels and HIF-1 transcriptional activity and sensitizes hypoxic colon adenocarcinoma cells to 5-fluorouracil. *Cancer Lett.* 2015;364. https://doi.org/10.1016/j.canlet.2015.05.008.
52. Scudiero DA, et al. Evaluation of a Soluble Tetrazolium/Formazan Assay for Cell Growth and Drug Sensitivity in Culture Using Human and Other Tumor Cell Lines. *Cancer Res.* 1988;48:4827–4833.